A detailed comparison of centrifugal sudden and J-shift estimates of the reactive properties of the N + N_2 reaction

Ernesto Garcia,[a] Carlos Sánchez,[a] Amaia Saracibar,[a] Antonio Laganà[b] and Dimitris Skouteris[b]

Received 28th July 2009, Accepted 29th September 2009
First published as an Advance Article on the web 27th October 2009
DOI: 10.1039/b915409d

An extended comparison of the reactive properties of the N + N_2 exchange reaction calculated on a non-collinear dominant potential energy surface using both a centrifugal sudden and a J-shift quantum method is reported. The choice of carrying out such an investigation for N + N_2 is motivated by the fact that the best available (and currently used for spacecraft re-entry simulations) computed set of kinetic data has been worked out using the low level J-shift approximation though based on exact quantum zero total angular momentum probabilities. The fact that our investigation is carried out for a heavy system and a potential energy surface free of wells in the strong interaction region minimizes the occurrence of tunnel, resonance and interference effects which would make the rationalization of the result difficult and the centrifugal sudden treatment less accurate. The study has provided evidence of two important limits of the J-shift approximation: the wrong determination of the maximum value of the total angular momentum quantum number J contributing to reactivity and the lack of deformation of the partial reactive probability dependence on energy at fixed J value. Accordingly, it has been found that the J-shift state-specific cross sections underestimate the corresponding CS values when the initial diatomic rotational energy is low while the situation reverses when the initial diatomic rotational energy is high.

1. Introduction

To obtain accurate quantum estimates of the state-specific cross sections and thermal rate coefficients of elementary reactions one has to first determine the corresponding set of exact probabilities. Most often the calculations of the required set of exact quantum probabilities are simply unmanageable even for the simplest reactive systems (as is the case of the atom–diatom ones) especially when the masses of the intervening atoms are heavy and/or the electronic structure is complex. In these cases, the only way out is to reduce the amount of memory and wall clock computing time by adopting approximate computational schemes decoupling the dependence of the probability on some parameters of the problem. However, the assumptions on which the adopted approximations rely need always be carefully pondered and the associated error systematically checked against more accurate results. This is of particular importance when, as is the case of the title reaction, little comfort is obtained from experimental data[1–3] and low level model treatments (though based on exact zero total angular momentum calculations of quantum reactive probabilities) are adopted to evaluate cross sections and thermal rate coefficients.[4–10]

Fortunately, some features of the N + N_2 system make it suited for high level quantum treatments. Although this will be dealt with in more details later on, it is worth mentioning at this point that N + N_2 is a sufficiently light and simple atom–diatom system to allow a rigorous close coupling expansion of the partial waves while, however, being free of very light atoms which generate highly structured and difficult to rationalize probability plots.

The high level quantum treatment we have considered to compare with the low level J-shift model[11,12] results adopted in the literature is the centrifugal sudden (CS) one[13,14] which drops from the Hamiltonian the centrifugal coupling term and keeps constant the projection of the total angular momentum $\boldsymbol{J}$ along the body-fixed (BF) Z axis. This allows decoupling of K (the discrete projection of $\boldsymbol{J}$ onto the BF quantization axis) exact quantum calculations at fixed J (the total angular momentum quantum number) into several fixed K ones at fixed J each of them not exceeding the memory size of the $J = 0$ run. The (very popular) mentioned J-shift model, instead, drastically reduces the calculations to the only (exact quantum) $J = 0$ probabilities which are properly shifted in energy in order to mimic the effect of increasing J. Clear examples of failure of the J-shift model have already been reported in the literature for systems containing hydrogen[15,16] and have been attributed to the property of light atoms of "feeling" the formation of wells in the energy adiabats.

An advantage of the title reaction for both aspects mentioned above is the fact that, as already mentioned before, it is not made of light atoms and that the potential energy surface (PES) adopted by us to carry out the dynamics calculations does not contain wells (after all, this makes the system also better suited for applying the CS method).

[a] *Departamento de Quimica Fisica, Universidad del Pais Vasco, 01006 Vitoria, Spain*
[b] *Dipartimento di Chimica, Università di Perugia, 06123 Perugia, Italy*

On the calculation of cross sections and thermal rate coefficients of the N + N_2 reaction there is a significant ongoing amount of research also because of their importance for modeling the spacecraft re-entry.[5–7,17,18] As a matter of fact, widely accepted now is the idea that, despite satisfactory agreement obtained between the values of the thermal rate coefficient[4,8,10,19–24] calculated on the collinear dominant LEPS PES[25] originally proposed for this reaction and the measured ones,[1–3] the LEPS potential energy surface is incorrect in the energy and geometry of the system at the saddle to reaction. Extended *ab initio* calculations[4,26,27] clearly indicate, in fact, that the energy at the saddle is higher and the geometry of the system is bent. This has prompted the fitting of some new PESs, the most used of which are L3,[28] WSHDSP[4,29] and L4.[30] On all these PESs exact quantum zero total angular momentum state-to-state reactive probabilities have been calculated and used to evaluate the thermal rate coefficients to be compared with the experiment using the already mentioned J-shift model.[4–10,31–34] This makes the calculated values to a large extent uncertain and undermines the meaning of their disagreement with the experiment. On the contrary, the comparison performed in our work represents the highest level analysis that could be performed using presently available computer facilities, also bearing in mind that it is carried out to assess the tools used to determine a suitable PES rather than produce a set of results on a solidly demonstrated accurate potential energy surface.

To carry out the calculations reported in this paper we made a combined use of the high performance platform MareNostrum of the Barcelona Supercomputing Centre[35] and of the distributed computing power of the segment of the production grid of EGEE[36] made available to the COMPCHEM virtual organization.[37,38]

The paper is, accordingly, organized as follows: in section 2 the details of the calculations are given, in section 3 the CS and J-shift quantum probabilities are analyzed and compared, in section 4 the comparison is extended to the CS and J-shift cross section values, and in section 5 some conclusions are drawn.

2. Details of the calculations

To compute the exact quantum three-dimensional state-specific reactive probability of atom–diatom reactions for a given value of the total angular momentum quantum number J, $P_{vj}^{J}(E)$, one takes the square modulus of the corresponding detailed $\boldsymbol{S}$ matrix element $S_{vjK,v'j'K'}^{Jp}(E)$:[39]

$$P_{vj}^{J}(E)=\frac{1}{(2K_{\max}+1)}\sum_{v'}\sum_{j'}\sum_{K=-K_{\max}}^{K_{\max}}\sum_{K'=-K'_{\max}}^{K'_{\max}}\sum_{p=0}^{1}|S_{vjK,v'j'K'}^{Jp}(E)|^{2} \tag{1}$$

where E is the total energy of the system, K is the body-fixed projection of the total angular momentum, p is the total parity, v and j are the initial vibrational and rotational quantum numbers, and $K_{\max}$ = min(j,J) (with priming referring, as usual, to final states). In this summation, for the particular case of the N + N_2 reaction, probabilities for even j' states contribute twice because the nuclear spin of the N atom is one,[40] *i.e.* a factor of 4/3 is applied if j' is even and a factor of 2/3 is applied if j' is odd.

From the partial state-specific probabilities the corresponding partial state-specific cross sections, $\sigma_{vj}^{J}(E)$, and the state-specific cross sections, $\sigma_{vj}(E)$, can be evaluated using the following expression:[39]

$$\begin{aligned}\sigma_{vj}(E)&=\sum_{J=0}^{J_{\max}}\sigma_{vj}^{J}(E)\\&=\sum_{J=0}^{J_{\max}}\frac{\pi}{k_{vj}^{2}}\frac{(2J+1)}{(2j+1)}(2K_{\max}+1)P_{vj}^{J}(E)\end{aligned} \tag{2}$$

where $k_{vj}^{2}=2\mu E_{\mathrm{tr}}/\hbar^{2}$ (in which E_{tr} is the relative collision energy and μ the reactant reduced mass) is the wavenumber of the system in the vj state. $J_{\max}$ represents the value of the total angular momentum quantum number beyond which no further reaction takes place.

According to the J-shift scheme, the J = 0 exact quantum detailed $\boldsymbol{S}$ matrix elements for a sufficiently wide energy interval and all the initial vibrational states relevant to the evaluation of the N + N_2 rate coefficients in the temperature interval spanned by the experiment were calculated first. From the calculated J = 0 quantum reactive probabilities, $P_{vj}^{J=0}(E)$, the J-shift state-specific probabilities, $P_{vj}^{*J}(E)$, were evaluated as follows:

$$P_{vj}^{*J}(E)=\frac{1}{(2K_{\max}+1)}\sum_{K=-K_{\max}}^{K_{\max}}P_{vj}^{J=0}(E-\Delta E^{JK}) \tag{3}$$

in which the energy shift ΔE^{JK} depends both on J and on K according to the relationship:

$$\Delta E^{JK}=\bar{B}J(J+1)+(A-\bar{B})K^{2} \tag{4}$$

that is based on the (approximate) assumption that the geometry of the system at the saddle is a symmetric top one. In eqn (4), $\bar{B}$ is defined as (B + C)/2 while A = 6.7 × 10^{-4} eV, B = 6.0 × 10^{-5} eV and C = 5.5 × 10^{-5} eV are the three rotational constants of the N_3 triatom at the saddle. As is apparent from eqn (4), the additional K term appearing in the J-shift correction for reactive systems having a bent geometry at the saddle further displaces to higher energy the large J partial probabilities.

To carry out a comparison with CS results, the calculations were performed for all the J > 0 (and all the related K) values at several rotational states of the ground vibrational level including the ones most populated at the temperatures of the experiment (j = 14 and j = 24). The great advantage of adopting the CS approximation is the possibility of calculating all the partial terms of eqn (2) in a simplified way. In fact, due to the decoupling of K, the total parity p (which selects the values of K to be coupled) has no effect and the related summation can be removed. In eqn (2) only the K positive projections are considered, because $S_{vjK,v'j'K'}^{J}(E)=S_{vj-K,v'j'-K'}^{J}(E)$ due to the symmetry of the N + N_2 system. Moreover, in the present CS calculation the approximation K' = K (as indicated later) is adopted and consequently the summation over K' can be removed.

The computational program used for our calculations is RWAVEPR,[41,42] a code based on the propagation of a complex wave-packet in time. To set up the initial wave-packet, Jacobi coordinates of the reactant arrangement are used. Then the wave-packet is represented in the product Jacobi coordinates of the channel of interest. The entire propagation is carried out using the product Jacobi coordinates. At each stage of the propagation, the overlap of the wave-packet with each of the open product channels is calculated. At the end of the propagation, the state-to-state $\boldsymbol{S}$ matrix elements for all open product channels and all energies are calculated using the overlap values calculated throughout the propagation by a half-Fourier transform as suggested by Gray and Balint-Kurti.[43]

The potential energy surface used is the L3 one[19] of the LAGROBO type[44–46] showing a saddle to reaction of 1.40 eV and almost the same bent transition geometry of WHSDSP and L4.

CS is itself an approximation. However, the CS approximation for the N + N_2 reaction is expected to work well over the whole range of coordinate values. One can, in fact, formulate the CS approximation in the asymptotic and the strong interaction regions. In the asymptotic region, where the potential is zero, an "average" value of the orbital l quantum number is assumed for all states with certain j and J quantum numbers. Since the rotational constant B goes to zero at infinity, the CS approximation holds good (all l states become degenerate and one is free to choose appropriate linear combinations to generate K states). In the strong interaction region, different K states are well separated from each other by the potential. Coriolis interactions are much weaker than the energy difference between K states and K remains a good quantum number. The problematic region is, instead, the intermediate one where the potential is not strong enough to separate K states from each other to a sufficient degree but the B rotational constant is high enough to cause a significant energy difference between l states (or to cause significant Coriolis coupling between K states). A rough estimate of the Coriolis matrix element (for low K and high j, J) is given by the product BJj (in the intermediate region one can assume that j is still a semi-good quantum number). Putting in the reduced mass of the N + N_2 system (and using example values of $j = 8$, $J = 70$), the Coriolis interaction energy is around $0.345/R^2$ eV (with R expressed in a_0). This term will reach appreciable values (more than 0.01 eV) at $R < 5.8a_0$. However, at such distances the N + N_2 potential angular anisotropy is 0.12 eV, a value sufficiently high to achieve separation of the K states.

As already mentioned, the initial wave-packet is set up in the Jacobi coordinates of the reactant arrangement while the product Jacobi coordinates of the channel of interest are used for time propagation. This implies that the initial K state is transformed into a linear superposition of K' product states. At this step the approximation $K' = K$ is introduced. The identity $K' = K$ is satisfied at the reactant asymptote. In fact, asymptotically, reactant and product Jacobi axes are either parallel or antiparallel (depending on the convention choice) and therefore if the K state can be described, as previously commented, by a combination of l (degenerate) states, K' will be described by the same (excluding the sign if reactant and product Jacobi axes are chosen antiparallel) combination of l states. This asymptotic regime is also satisfied at $R = 8.5a_0$, where the initial wave-packet is initially placed and the transformation to product Jacobi coordinates is performed. In fact, at this distance the Coriolis coupling (estimated by the product BJj) remains lower than 0.01 eV for values of the product Jj as high as 1200, covering practically all the J values contributing to the reaction at the reactant rotational states considered.

A crucial aspect for the success of the related extended computational campaign was the exploitation of two types of massively concurrent platforms. One was the distributed memory Marenostrum machine[35] using GridSuperScalar (GSS).[47] GSS parallelizes at runtime and at task level sequential applications and executes them on a computational grid. In our case it was possible to parallelize the application as a set of coarse grained tasks. The other platform used was the segment of the production grid infrastructure of EGEE[36] accessible to the COMPCHEM virtual organization.[37,38] In this case, we designed a workflow articulated in three steps.[24] The first step creates the list of machines selected to run the jobs. The second step creates all the needed information about the jobs (*e.g.*, the initial quantum labels v,j,J,K,p and the total energy range). Then a sequence of "job submission-check-retrieve-rerun" is iterated until completion of the set of tasks. The submission procedure implies sending of both the specific input file and the executable program to an available machine. The check is performed periodically and controls the status of the jobs over the grid. According to the status of the job the output files are retrieved (correct completion) or re-sent (failure).

Computed $\boldsymbol{S}$ matrix elements are stored in a repository for subsequent use and analysis. The calculation of the reactive scattering properties is, in fact, carried out offline using dedicated programs.

3. CS and J-shift partial probabilities

As already mentioned CS partial state-specific probabilities, $P^J_{vj}(E)$, were calculated at $v = 0$ and various rotational levels by increasing J up to a value of 105 (the maximum value of J contributing to the reaction) and E from 1.260 to 2.300 eV in steps of 0.001 eV. For $J \leq j$ calculations were performed at all values of J while for $J > j$ calculations were performed every 5 units. In all cases, however, all the K positive projections of $\boldsymbol{J}$ were considered.

For illustrative purposes, the CS and J-shift $P^J_{v=0,j}(E)$ values calculated at different total energies are plotted in Fig. 1 as a function of J. As shown in the figure, the maximum value of J actually contributing to the reaction (J_{max}) decreases with the initial rotational state and increases with the total energy. This features are predicted by both CS and J-shift approximations. However, the J-shift values underestimate (overestimate) the CS ones when the rotational excitation is low (high).

An additional discrepancy between the CS and J-shift results is the appearance of some peculiar structures in the CS $P^J_{v=0,j}(E)$ plots. In fact, at $j = 0$ and low total energy (bottom leftmost panel) the CS $P^J_{v=0,j=0}(E)$ curve has a maximum at $J = 0$ and then decreases smoothly as J increases

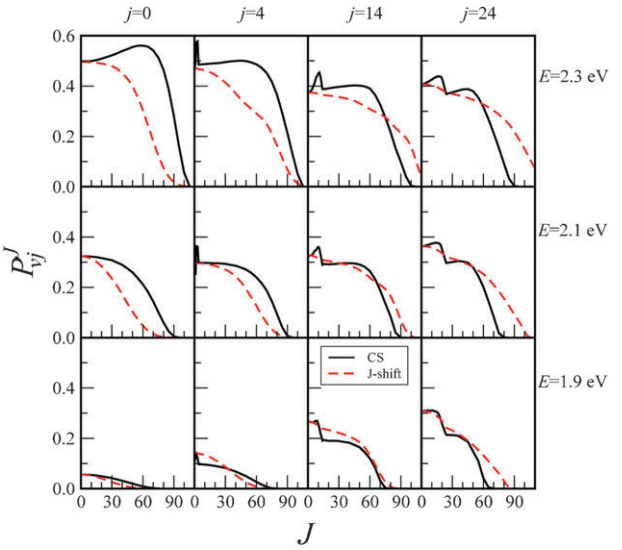

Fig. 1 CS $P_{vj}^J(E)$ (solid lines) and J-shift $P_{vj}^{*J}(E)$ (dashed lines) partial state-specific probabilities calculated at $v = 0$ and $j = 0$, 4, 14 and 24 plotted for three different values of the total energy as a function of J.

(in agreement with the basic J-shift concept that an increase of J subtracts energy available for reaction). On the contrary, at the highest energy considered (top leftmost panel), the value of the CS $P_{v=0,j=0}^J(E)$ increases in going from $J = 0$ to $J = 60$ at which a maximum occurs. Then it suddenly decreases for higher J values. When N_2 is rotationally excited CS $P_{v=0,j}^J(E)$ has a structure at $J < j$ while it keeps a shape similar to that at $j = 0$ at $J > j$. At the same time, the absolute value of $P_{v=0,j}^J(E)$ increases with j at low total energy (bottom panels) and decreases with it at high total energy (top panels). The structure associated with $J < j$ can be understood as a stereodynamical bias of the reactive processes induced on the relative atom–diatom orientation by the condition $K_{max} = \min(J,j)$ when the saddle to reaction is bent. However, since this effect, though being non-negligible, occurs only at low J values (and, therefore, scarcely impacts the final value of the cross section), it will not be discussed any further in this paper.

On the other hand, the dependence on J of the J-shift partial probabilities $P_{v=0,j}^{*J}(E)$ well illustrates the result of adopting the J-shift model. For all initial rotational states, the J-shift curves have a monotonic decreasing evolution with J. This means that the stereodynamical effects characterizing the low J probability values go completely missed confining the possible validity of J-shift approaches only to largely averaged quantities. Significant differences are also observed when comparing CS and J-shift results at low and high rotational excitation. At $j = 0$ the J-shift probability decreases faster than the CS one. This effect, which is small at low total energy, becomes significant at high energy making the J-shift model underestimate reactivity. However, the situation reverses as j increases indicating that the J-shift results may not be considered either a lower or an upper limit of the CS ones. The discrepancies found between CS and J-shift results imply that when increasing J the CS probabilities deviate significantly from the ones derived from $P_{v=0,j}^{J=0}(E)$ by the energy shifting of eqn (4).

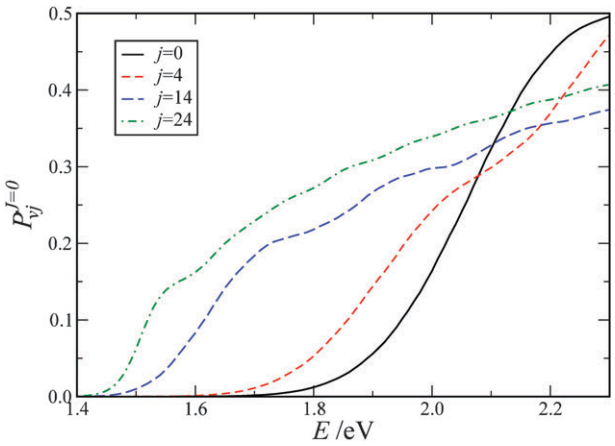

Fig. 2 Zero total angular momentum partial state-specific probabilities $P_{vj}^{J=0}(E)$, calculated at $v = 0$ and $j = 0$ (solid line), 4 (dashed line), 14 (long dashed line) and 24 (dotted dashed line) plotted as a function of the total energy E.

To understand the dependence on J of the J-shift partial probabilities, the reference to the (exact) $J = 0$ probabilities is due. The resulting values, plotted in Fig. 2 as a function of the total energy, show for the initial rotational states considered a behaviour typical of the reactive probabilities of barrier controlled reactions. The rotational energies of 0.005, 0.052 and 0.148 eV associated with the considered $j = 4$, 14 and 24 rotational states, respectively, are clearly insufficient to drive the system over the saddle that is 1.40 eV high. For this reason they show an appreciable energy threshold and a subsequent increasing trend with energy, that is easily reconciled with the behaviour of a hard sphere model.

Yet, some important differences can be singled out when comparing the detail of the probability curves for different rotational states of the reactants. In fact, as is apparent from Fig. 2, threshold energy decreases as rotational excitation increases. This indicates an effective use of the rotational energy to promote reaction. As a matter of fact, the threshold energy for $j = 24$ (for which the fraction of energy allocated in internal modes is large) is about 0.3 eV lower than that for $j = 0$ despite the fact that the associated rotational excitation amounts only to 0.148 eV. This feature was attributed in ref. 8 to the bent geometry of the saddle in the L3 PES as opposed to the scarce effectiveness of the internal energy found for the collinear dominant LEPS PES. Such a clear cut example is confined, however, to the threshold region. At higher energies, a sharper rise of the probability for lower rotational states makes its value much larger at $j = 0$ and 4 than at $j = 14$ and 24. Moreover, the $j = 14$ and 24 plots are roughly parallel in the whole energy interval indicating that, at high rotational excitation, the modification of the probability plot is close to an energy shifting.

To understand in more detail the reasons for the inadequacy of the J-shift model to reproduce the CS $P_{v=0,j}^J(E)$ curves we have studied also the dependence on E, J and K of the single K contributions to the partial state-specific probabilities. For illustrative purposes, the mentioned contributions calculated at $v = 0$ and $j = 24$ are shown in Fig. 3. As is apparent from the figure, J-shift probabilities well reproduce the CS ones at

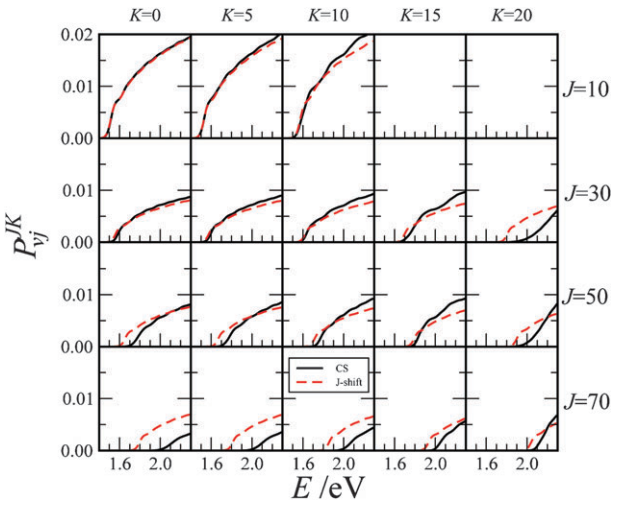

Fig. 3 CS $P_{vj}^{J}(E)$ (solid lines) and J-shift $P_{vj}^{*J}(E)$ (dashed lines) single K partial state-specific probabilities calculated at $v = 0$ and $j = 24$ plotted as a function of the total energy, E.

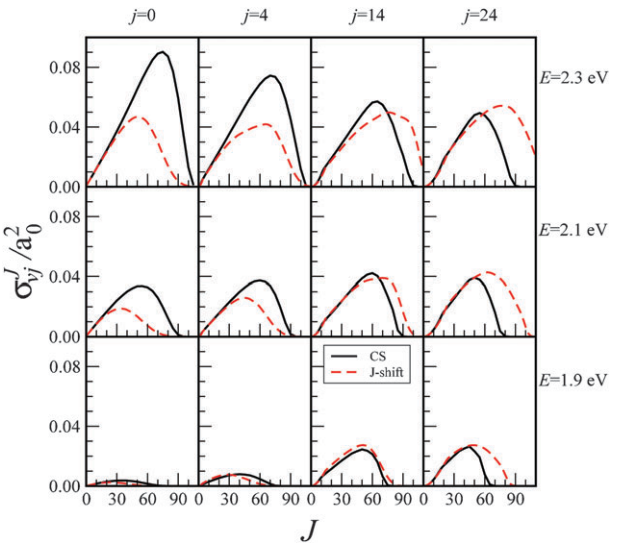

Fig. 4 CS $\sigma_{vj}^{J}(E)$ (solid lines) and J-shift $\sigma_{vj}^{*J}(E)$ (dashed lines) partial state-specific cross sections, calculated at $v = 0$ and $j = 0$, 4, 14, 24 plotted for three different values of the total energy as a function of J.

$K = 0$ and relative low values of J ($J = 10$ and 30). Larger differences show up for $J = 50$ and, as K increases, the agreement is even worse and deteriorates with energy. For large J values the disagreement is strong also at $K = 0$. The use of the J-shift model, therefore, does not find any plausible justification but in the computer time saving that nowadays with the advent of computing grid is less of an issue.

4. CS and J-shift cross sections

With the condition stated in the previous section we moved to the analysis of the state-specific cross sections starting from the partial ones. As is apparent from eqn (2), the main factor involved in the calculation of the partial cross sections from partial probabilities is the factor $(2J + 1)$, which privileges the reactivity at high angular momentum quantum numbers. Moreover, the factor $(2K_{max} + 1)/(2j + 1)$ amplifies the effect since its value is one when $J \geq j$ and lower than one when $J < j$.

The values of the CS partial state-specific cross section, $\sigma_{v=0,j}^{J}(E)$, corresponding to those of the partial probabilities of Fig. 1 are reported in Fig. 4. As is apparent from the figure, in all cases the partial cross section terms are small at $J = 0$. Then they increase with J to reach a maximum and to rapidly decrease to zero immediately afterwards. However, the value of J at which the maximum occurs as well as the slopes of increase and decrease with J, depends significantly on the initial rotational and total energy of the system. At $E = 2.3$ eV, for example, the partial cross section has its largest maximum at $j = 0$ that is located at $J = 75$. As the energy decreases, the $j = 0$ maximum lowers and moves to smaller values of J. As an example, at $E = 2.1$ eV the maximum is located at $J = 55$, 20 units lower than that at $E = 2.3$ eV. An increase of the rotational excitation of the reactants, however, does not always have the same effect. In fact, at the highest total energy considered, an increase of rotational energy results in a decrease in the height of the maximum and its shift to lower values of J (for example, at $j = 14$ the maximum is located at $J = 65$). On the contrary, at low energy, the maximum of the partial cross section increases and moves to larger values of J as j gets larger (for example, the maximum moves from $J = 35$ when $j = 0$ to $J = 50$ when $j = 14$ at $E = 1.9$ eV). Both the increasing and the decreasing trend tend to vanish at the highest rotational state. This figure also confirms the practical irrelevance of the structures arising at $J < j$ to the end of determining the value of the cross section and the dependence of the CS results on the specific reactant state.

In Fig. 4 the J-shift partial state-specific cross sections, $\sigma_{v=0,j}^{*J}(E)$, are also shown. Their comparison with CS values tells us that, despite the similarities in shape, they largely underestimate the CS values at low j values while they overestimate the ones at high j values, especially at large total energy.

This is indeed what was found when calculating and comparing CS $\sigma_{vj}(E)$ and J-shift $\sigma_{vj}^{*}(E)$ state-specific cross sections. Fig. 5 plots both of them as a function of E (excitation function). The excitation function (the dependence of the cross section on energy) shows for all the initial rotational states the typical behaviour of reactions occurring *via* a barrier surmounting. However, significant differences can be appreciated for both the various rotational states and the approximations used for the calculations.

CS cross sections exhibit a clear dependence on the rotational energy. In fact, the threshold energy of the reaction moves to lower values as the rotational excitation increases. This implies, as already mentioned, an efficient use of the rotational energy for promoting the reactivity associated with the bent geometry of the saddle. Therefore, the shift in energy for the threshold depends on the rotational state involved. The threshold energy moves slightly when going from $j = 0$ to $j = 4$ (as expected because of the modest difference in energy). On the contrary, when moving from $j = 4$ to $j = 14$ the effect is more substantial (as expected from the larger difference in rotational energy). However, the results show a saturation point. In fact, when the rotational excitation increases from

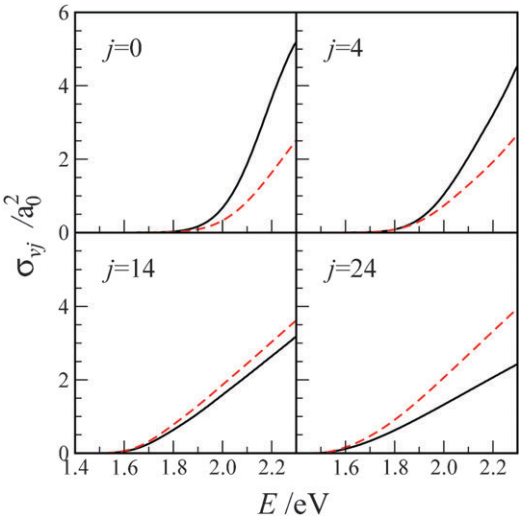

Fig. 5 CS $\sigma_{vj}(E)$ (solid lines) and J-shift $\sigma^{*}_{vj}(E)$ (dashed lines) state-specific cross sections calculated at $v = 0$ and $j = 0, 4, 14, 24$ plotted as a function of the total energy E.

$j = 14$ to $j = 24$ (which corresponds to an ever larger increase in rotational energy), the threshold hardly decreases implying that above a certain value of the rotational energy no further contributions to reactivity are obtained. On its side, the slope of the past-the-threshold increasing trend of the reactivity with energy depends significantly on the rotational energy. As a matter of fact, the lower the rotational energy (and the higher the threshold) the larger the positive slope. This trend results in an inversion of the state leading to the largest cross section at high energy, meaning that there the translational energy becomes more efficient than the rotational one in promoting the reaction.

J-shift calculations reproduce the threshold energy predicted by the CS ones. However, the dependence of the slope on the J-shift excitation function is clearly weaker than that of the CS one. As a matter of fact, the slope is almost invariant with j leading to the already mentioned shift from an underestimation to an overestimation of the CS cross section in going from low to high rotational excitation.

5. Conclusions

The possibility of relying on suitable model treatments when dealing with the quantum calculations of the reactive properties of heavy atom–diatom chemical systems (as N + N_2) is a clear advantage in trying to reduce the related computational burden. In this paper, the popular J-shift scheme, often adopted to extrapolate to large J values the results of $J = 0$ exact quantum calculations, and its application to the N + N_2 system have been discussed. The evaluation of the accuracy of the model has been carried out by comparing the results obtained using a standard wave-packet approach to calculate centrifugal sudden $\boldsymbol{S}$ matrix elements with those obtained using only its $J = 0$ subset and then extrapolating them to J values as large as 105 using a J and K dependent energy shift. In this way, we have been able to point out that the results of the J-shift model treatment represent neither an upper nor a lower limit to the CS ones. It was found, in fact, that the first limitation of the J-shift model is the wrong determination of J_{max}. This inaccuracy is, moreover, accompanied by a second significant inaccuracy concerned with the wrong dependence of the plots of the calculated probabilities on energy or J. As a matter of fact the J-shift excitation function depends on the initial diatomic rotational energy more weakly than the CS one, leading to state-specific cross sections higher (smaller) than the CS values at low (high) j.

Acknowledgements

Partial financial support from MICINN (CTQ-2008-02578/BQU), MIUR, EGEE III and ARPA Umbria is acknowledged. This work has been carried out also as part of the activities of the cooperation scheme of the QDYN working group of the COST CMST European Cooperative Project CHEMGRID (Action D37). Computational assistance and resources were provided also by the SGI/IZO-SGIker at the University of the Basque Country and by the Spanish Supercomputing Network (BSC-RES).

References

1 R. A. Back and J. Y. P. Mui, *J. Phys. Chem.*, 1962, **66**, 1362.
2 A. Bar-Nun and A. Lifshitz, *J. Chem. Phys.*, 1967, **47**, 2878.
3 R. K. Lyon, *Can. J. Chem.*, 1972, **50**, 1437.
4 D. Wang, J. R. Stallcop, W. M. Huo, C. E. Dateo, D. W. Schwenke and H. Partridge, *J. Chem. Phys.*, 2003, **118**, 2186.
5 D. Wang, J. R. Stallcop, C. E. Dateo, D. W. Schwenke and W. M. Huo, *42nd AIAA Aerospace Science Meeting*, Paper 2004-0337, 2004.
6 R. Jaffe, D. W. Schwenke, G. Chaban, G. Chaban, R. Jaffe and D. W. Schwenke, *46th AIAA Aerospace Science Meeting*, Paper 2008-1208, 2008.
7 G. Chaban, R. Jaffe and D. W. Schwenke, *46th AIAA Aerospace Science Meeting*, Paper 2008-1209, 2008.
8 E. Garcia, A. Saracibar, A. Laganà and D. Skouteris, *J. Phys. Chem. A*, 2007, **111**, 10362.
9 A. Laganà, N. Faginas-Lago, F. Huarte-Larrañaga and E. Garcia, *Phys. Scr.*, 2008, **78**, 058116.
10 S. Rampino, D. Skouteris, A. Laganà, E. Garcia and A. Saracibar, *Phys. Chem. Chem. Phys.*, 2009, **11**, 1752.
11 J. M. Bowman, *J. Phys. Chem.*, 1991, **95**, 4960.
12 J. M. Bowman, *Lect. Notes in Chem.*, 2000, **75**, 101.
13 R. T. Pack, *J. Chem. Phys.*, 1974, **60**, 633.
14 Y. Sun, R. S. Judson and D. J. Kouri, *J. Chem. Phys.*, 1989, **90**, 241.
15 V. Piermarini, S. Crocchianti and A. Laganà, *J. Comput. Methods in Sciences and Engineering*, 2002, **2**, 361.
16 M. H. Alexander, private communication.
17 I. Armenise, M. Capitelli, E. Garcia, C. Gorse, A. Laganà and S. Longo, *Chem. Phys. Lett.*, 1992, **200**, 597.
18 I. Armenise, M. Capitelli, R. Celiberto, G. Colonna, C. Gorse and A. Laganà, *Chem. Phys. Lett.*, 1994, **227**, 157.
19 A. Laganà and E. Garcia, *J. Phys. Chem.*, 1994, **98**, 502.
20 A. Laganà, G. Ochoa de Aspuru and E. Garcia, *AIAA Journal*, 1994, **94**, 1986.
21 F. Esposito and M. Capitelli, *Chem. Phys. Lett.*, 1999, **302**, 49.
22 N. Faginas-Lago, A. Laganà, R. Gargano and P. R. P. Barreto, *J. Chem. Phys.*, 2006, **125**, 114311.
23 N. Faginas-Lago and A. Laganà, *Lect. Series on Computer and Computational Sci.*, 2006, **7**, 297.
24 A. Saracibar, C. Sánchez, E. Garcia, A. Laganà and D. Skouteris, *Lect. Notes Comput. Sci.*, 2008, **5072**, 1065.
25 A. Laganà, E. Garcia and L. Ciccarelli, *J. Phys. Chem.*, 1987, **91**, 312.
26 C. Petrongolo, *J. Mol. Struct.*, 1988, **175**, 215.
27 C. Petrongolo, *THEOCHEM*, 1989, **202**, 135.

28 E. Garcia and A. Laganà, *J. Phys. Chem. A*, 1997, **101**, 4734.
29 J. R. Stallcop, H. Partridge and E. Levin, *Phys. Rev. A: At., Mol., Opt. Phys.*, 2001, **64**, 042722.
30 E. Garcia, A. Saracibar, S. Gómez-Carrasco and A. Laganà, *Phys. Chem. Chem. Phys.*, 2008, **10**, 2552.
31 D. Wang, W. M. Huo, C. E. Dateo, D. W. Schwenke and J. R. Stallcop, *Chem. Phys. Lett.*, 2003, **379**, 132.
32 D. Wang, W. M. Huo, C. E. Dateo, D. W. Schwenke and J. R. Stallcop, *J. Chem. Phys.*, 2004, **120**, 6041.
33 N. Faginas-Lago, F. Huarte-Larrañaga and A. Laganà, *Chem. Phys. Lett.*, 2008, **464**, 249.
34 S. Rampino, D. Skouteris, A. Laganà and E. Garcia, *Lect. Notes Comput. Sci.*, 2008, **5072**, 1081.
35 Barcelona Supercomputing Centre—Red Española de Supercomputación, http://www.bsc.es.
36 Enabling Grids for *E*-Science in Europe (EGEE), http://www.eu-egee.org.
37 COMPCHEM Virtual Organization, http://www.compchem.unipg.it.
38 A. Laganà, A. Riganelli and O. Gervasi, *Lect. Notes Comput. Sci.*, 2006, **3980**, 665.
39 F. J. Aoiz, V. Sáez-Rábanos, B. Martínez-Haya and T. González-Lezana, *J. Chem. Phys.*, 2005, **123**, 094101.
40 G. Herzberg, *Molecular Spectra and Molecular Structure. I Spectra of Diatomic Molecules*, Van Nostrand, New York, 1950.
41 D. Skouteris, L. Pacifici and A. Laganà, *Mol. Phys.*, 2004, **102**, 2237.
42 D. Skouteris, A. Laganà, G. Capecchi and H.-J. Werner, *Int. J. Quantum Chem.*, 2004, **96**, 562.
43 G. G. Balint-Kurti and S. K. Gray, *J. Chem. Phys.*, 1998, **108**, 950.
44 A. Laganà, *J. Chem. Phys.*, 1991, **95**, 2216.
45 E. Garcia and A. Laganà, *J. Chem. Phys.*, 1995, **103**, 5410.
46 A. Laganà, G. Ochoa de Aspuru and E. Garcia, *J. Chem. Phys.*, 1998, **108**, 3886.
47 R. M. Badia, J. Labarta, R. Sirvent, J. M. Pérez, J. M. Cela and R. Grima, *J. Grid Comput.*, 2003, **1**, 151.

